TEST Engineering & Management

January - February 2020
ISSN: 0193 - 4120 Page No. 11323 - 11332

Pathological Brain Tumor Detection Using CLAHE and LS-SVM

Machiraju Jaya Lakshmi[1], Dr. S.Nagaraja Rao[2]
[1]Research scholar, JNTUA, Anantapuramu, India,
[2]Professor & HOD, Department of ECE, G.Pulla Reddy Engineering College (Autonomous), Kurnool, India.
[1]jayaraju15kumar@gmail.com, [2]hodece@gprec.ac.in.

Article Info
Volume 82
Page Number: 11323 - 11332
Publication Issue:
January-February 2020

Abstract
The segmentation, early detection and removal of infected tumor region from Magnetic resonance images is a main problem but tedious and time-consuming task conducted by radiologists and their precision depends only on their knowledge. To solve these constraints, it becomes very important to use computer-aided technology. In this study, the medical image involves improving performance and reducing complexity. This paper proposes an efficient PBDS based on MR images that significantly enhances recent results. To improve the quality of input of MR images, the proposed system uses CLAHE. Subsequently segmented using OTSU and K means segmentation methods. On the segmented image, morphological operations are performed to obtain the information about the tumor area, size and density. Using a discrete wavelet transform (DWT) strategy, the segmented image is then transformed to extract features. Subsequently, the PCA approach reduce the dimensionality of the features. The reduced features were submitted to a Least square support vector machine (LS-SVM). The strategy of 5×k-fold stratified cross validation (SCV) test has been carried out to enhance LS-SVM generalization. We performed our proposed methods with four different kernels and found that the GRB kernel has the highest classification accuracy of 99.38%. The LIN, HPOL, and IPOL kernel achieves 95%, 96.88%, and 98.12%, respectively. We also compared our method to those from literatures in the last decade, and the results showed our CLAHE+DWT+PCA+LS-SVM with GRB kernel still achieved the best accurate classification results It could be applied to the field of MR brain image classification and can assist the doctors to diagnose where a patient is normal or abnormal to certain degrees at the early stage.

Keywords: *K-means, Brain tumor, classification, segmentation, image de-noising, principal component analysis (PCA), Discrete wavelet transform (DWT), Least square support vector machine (LS-SVM).*

Article History
Article Received*: 18 May 2019*
Revised*: 14 July 2019*
Accepted*: 22 December 2019*
Publication*: 21 February 2020*

I. INTRODUCTION

Over the past decades, morality rates among people with different age groups rise sharply across the globe due to brain diseases. There are different types of brain diseases, such as cerebrovascular diseases (stroke), neoplastic diseases (brain tumor), infectious diseases, and degenerative diseases, all of which could lead to individual death. Therefore, the development of pathological brain detection system (PBDS) is of great importance for early of the brain diseases identification. This development's main objective is to arrive at right and quick clinical decisions. A modality of medical imaging called magnetic resonance imaging (MRI) is widely used in PBDS because of its benefit of providing significant knowledge about soft tissue of the human brain [1]. Moreover, MRI is a non-invasive and faster for medical imaging compared to other modalities such as X-ray and CT scan. However, manual interpretation becomes more difficult due to

January - February 2020
ISSN: 0193 - 4120 Page No. 11323 - 11332

high requirement of data storage of MR images. Moreover, manual interpretation is a costly, troublesome and time-consuming task [2]–[4]. To counter these problems, automated pathological brain detection systems (PBDSs) need to be built using dedicated computer systems that can assist radiologists to implementing corrective measures for early treatment of patients with ailing disease.

A lot of work has been done to develop numerous PBDSs through MR images over the past decade [5]. Developing an optimal PBDS however still needs potential improvements. We summarize some important earlier developments in PBDS in the following.The forebears, Chaplot et al. [6], suggested a two dimensional discrete wavelet transform (2D

DWT) features based PBDS technology. In this approach the Self-organizing map (SOM) and SVM are used separately as classifiers. El-Dahshan et al. [7] later introduced a 2D DWT based hybrid approach and two different classifiers such as k-nearest neighbor (k-NN) were used to minimize the principal component analysis (PCA) of dimensionality features. In addition, the authors in [1], [8], [9] proposed various PBDSs with the aid of classifiers such as FNN and BPNN optimized by gradient based and population-based optimization schemes such as scaled conjugate gradient (SCG), adaptive chaotic particle swarm optimization (ACPSO) and scaled chaotic artificial bee colony (SCABC).In [2], the authors suggested a PBDS in which the features are extracted from ripplet transform (RT) and then subjected to PCA for reduction in dimensionality. We finally applied least squares SVM (LS-SVM) to classify them. In [5], On the other hand, the authors have proposed a scheme where DWT and PCA are used for extraction and reduction of features before the use of the feedback pulse coupled neural network (FPCNN). Finally, they applied classifier FP-ANN. The stationary wavelet transform (SWT) and PCA based functions are derived in [10]. Generalized eigenvalue proximal SVM (GEPSVM) is used for classification. Subsequently, Zhang et al. [11] have proposed a PBDS in which two different types of entropies, namely Shannon entropy (SE) and Tsallis entropy (TE) are determined from the sub-bands of discrete wavelet packet transform (DWPT) and are used as features. Finally, GEPSVM is applied for classification. While the wavelet entropy features are added to a Naive Bayes classifier (NBC) in [12] .Later, Wang et al. [13] suggested a PBDS in which the features of fractional Fourier entropy (FRFE) are extracted and then twin SVM (TSVM) classifier is employed for classification. On the other hand, in [14], Hu moment invariants (HMI) and wavelet entropy (WE) features are used and eventually a GEPSVM and RBF classifier is applied. Nayak et al. [3] later proposed a scheme in which 2D DWT is used for extraction of features, while probabilistic PCA (PPCA) and AdaBoost with random forests (ADBRF) are harnessed for feature reduction and classification respectively. The variance and entropy (VE) values of a dual-tree complex wavelet transform (DTCWT) are then used as features in [15], and both GEPSVM and twin SVM (TSVM) are used as the classifier.

Therefore, instead of standard SVM, a least square SVM (LS-SVM) classifier is used which has the advantage of minimizing the computational costs by solving a set of linear equations. In Addition, contrast limited adaptive histogram equalization (CLAHE) and principal component analysis (PCA) are used for input MR image preprocessing and dimensionality reduction, respectively, of features extracted from DWT. It should be noted that the methods chosen are of a general nature and not limited to pathological brain detection alone, they can also be extended to any task of pattern recognition.

In addition, it has been found that few PBDSs need a large number of features and therefore a scope exists to restrict the requirement of the function without losing the accuracy. We propose a novel PBDS with the following characteristics.

- Pre-processing using CLAHE.
- To segment the pre-processed image using OTSU and K means clustering method.
- To measure the area, density, dilution amount used morphological operation.

TEST Engineering & Management

January - February 2020
ISSN: 0193 - 4120 Page No. 11323 - 11332

- DWT strategy is harnessed as feature extractor.
- To reduce the dimensionality PCA method is used.
- A new learning algorithm known as least square support vector machine (LS-SVM)is used to address the problems of conventional learning algorithms.
- Extensive experiments are carried out in order to validate the proposed scheme,. In this context, the scheme is compared with existing methods with respect in terms of accuracy.

II. DATA SET

Datasets consists of T2-weighted MR brain images in axial plane and 256 × 256 in-plane resolution, Downloaded from the Harvard Medical School website (URL: http://med.harvard.edu/AANLIB/), OASIS dataset (URL: http:// www.oasis-brains.org/), and ADNI dataset (URL: http://adni.loni.ucla.edu/). As T2 images are of higher-contrast and clearer vision compared to T1 and PET modalities, we select T2 model. The abnormal brain MR images of the dataset consist of the following diseases: meningioma, glioma, Alzheimer's disease, sarcoma, Alzheimer's disease plus visual agnosia, Pick's disease, and Huntington's disease. The samples of each disease are illustrated in Fig. 1.

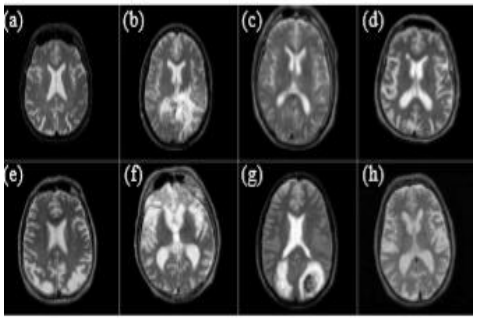

Figure1. Sample of brain MRIs:(a) normal brain;(b) glioma; (c) meningioma; (d) Alzheimer's disease; (e) Alzheimer's disease with visual agnosia; (f) Pick's disease; (g) sarcoma; (h) Huntington's disease.

We selected 20 images randomly for every type of brain. Because, there is one type of normal brain and seven types of abnormal brain in the dataset, 160 images are selected consisting of 20 normal and 140 abnormal brain images. A normal human brain's notable feature is the symmetry it exhibits in the axial and coronal images. Asymmetry strongly indicates abnormality in an axial MR brain image. As a result, symmetry in axial MR images is an important feature to be considered when deciding whether the MR image at hand is of a normal or an abnormal brain. The configuration of the training images and validation images is shown in Table 1 with 5-fold cross validation.

Table 1. Setting of training and validation images (5-fold stratified cross validation).

Total No. of images	Training (128)		Validation (32)	
	Normal	Abnormal	Normal	Abnormal
160	112	4	28	16

III. PROPOSED METHOD

The proposed PBDS involves four stages, including pre-processing using CLAHE, segmentation is done using OTSU and K means clustering method, feature extraction using DWT, PCA used for dimensionality reduction, and classification using LS-SVM. The system input is an MR image, and the output is the class label (healthy or pathological). The detailed block diagram of the proposed PBDS is depicted in Figure 2. For brief, all the four steps are delineated below.

January - February 2020
ISSN: 0193 - 4120 Page No. 11323 - 11332

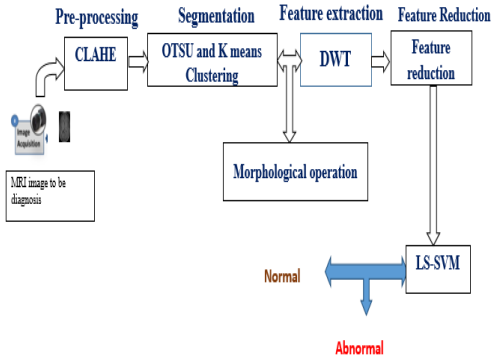

Figure 2. Proposed scheme Block diagram

A. *Pre-processing using CLAHE*

Acquired brain MR images need pre-processing to improve their quality, resulting in better features extraction. A popular technique called contrast limited adaptive histogram equalization (CLAHE) has therefore been utilized in this work, as it is found that most of the images in the datasets considered in this work are of low-contrast. CLAHE is an adaptive histogram equalization (AHE) variant that calculates an intensity histogram in each pixel-centered contextual region. Then, the pixel intensity in its local histogram becomes a value based on the pixel intensity level within the display range [17]. Unlike AHE, CLAHE prevents the over-enhancement of noise and diminishes the edge shadowing effect by limiting the contrast enhancement of AHE [16]. CLAHE restricts the amplification by clipping the histogram to a predefined value, called clip limit, before computing the cumulative distribution function (CDF). Therefore, it is desirable not to discard the parts of the histogram that exceeds the clip limit, but to redistribute it equally among all histogram bins. When During enhancing MR images with CLAHE the images are divided into different non-overlapping regions of nearly equal sizes. Then, the histogram is determined and equalized for each region by using CDF estimate [18]. The following describes the equalization procedure.

Let P and L be the number of pixels and grayscales respectively in each region, and $h_{i,j}(l)$, for $l=1,2,...,L-1$ be the histogram of (i,j) region. Then, the CDF scaled by (L−1) for grayscale mapping is defined as

$$F_{i,j}(l) = \frac{(L-1)}{P} \cdot \sum_{z=0}^{l} hi,j(z) \quad (1)$$

However, the main issue with equalization of histogram is that the region contrast is increased to its maximum. The maximum slope s_{max} of (1) is therefore limited to a desired maximum slope so as to limit the contrast to a desired level. This is done with the use of a clip limit, β which clips all histograms. Next, β is based on a clip factor, α (in %) and is given as

$$\beta = \frac{P}{L}\left[1+\frac{\alpha}{100}(s_{max}-1)\right] \quad (2)$$

Since the clip factor α ranges from 0 to 100, the maximum slope varies from 1 to s_{max} in each mapping. Once β is obtained, each histogram is redistributed once β is collected so that its height does not exceed β. Then the CDF is calculated for grayscale mapping, from limited histograms resulting from the contrast. Subsequently, the mapping results from the nearest regions are combined using bilinear interpolation to map a pixel, which in turn eliminates the artificially induced boundaries. It should be worth mentioning that the proper parameter setting of CLAHE strongly influences the result.

B. *OTSU and K-means clustering for segmentation*

The Otsu's objective function is equivalent to the multilevel thresholding method of K means [19]. Both of them are based on the same principles of reduce the variance within the class. The Otsu method also operates on global thresholding, while the K means method work on the local thresholding. Before running, the Otsu method requires a gray level histogram to be computed while K means does not need a gray level histogram to be calculated before running. All methods produce a good segmentation performance, but K means comparatively giving Otsu better results. Otsu method takes comparatively more time and makes the algorithm more complex.

C. *Wavelet-based feature extraction*

Wavelets are mathematical functions that decompose data into components of different frequency and then analyze each component with a resolution corresponding to its scale. Wavelets have emerged as powerful new methods to analyzing

TEST Engineering & Management

January - February 2020
ISSN: 0193 - 4120 Page No. 11323 - 11332

large datasets. The Fourier transform provides image representation based only on its information about frequencies. Therefore this representation is not localized spatially, while the wavelet functions are localized in space. The Fourier transform decomposes a signal into a frequencies spectrum while the wavelet analysis decomposes a signal into a hierarchy of scales ranging from the coarset scale. Consequently, Wavelet transform, which provides representation of an image at different resolutions, is a better tool for extraction of features.

The DWT is a wavelet transform an implementation that uses a discrete set of the wavelet scales and translation following certain defined rules. The wavelet transformation must be discretized, for practical computations. The parameter(s) of the scale (are) on a logarithmic grid discrete. The translation parameter (t) is then discretized with respect to the scale parameter, i.e. sampling is performed on the dyadic (as the base of the logarithm is usually chosen as two) sampling grid. The discrete parameters scale and translation are given by, $s=2^{-m}$ and $t=n.2^{-m}$, where m,n ϵ Z, the set of all integers. Thus, wavelet functions family is defined in Eq. (3),

$$\Psi_{m,n}(t)=2^{m/2}\psi(2^{m}t-n) \quad (3)$$

The wavelet transforms a signal x (t) into a family of wavelets for synthesis as shown in Equations below. (4) and (5),

$$x(t)=\sum_m \sum_n \psi_{m,n}(t) C_{m,n} \quad (4)$$

where, $C_{m,n}=x(t)\,\psi_{m,n}(t)$ (5)

DWT in two dimensions In case of images, the DWT is applied separately to each dimension. This results in an image Y being decomposed into a first level approximation component Y^1_a, and detailed components Y^1_h, Y^1_v and Y^1_d; corresponding to horizontal, vertical and diagonal details [20]. Fig. 3 depicts the process of decomposition of the image into approximate and detailed components.

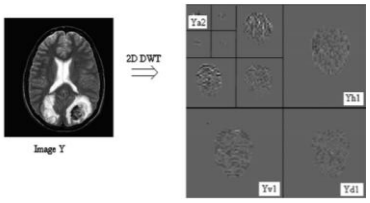

Figure 3. Wavelet transform of an image Y up to level two.Y1a andY2a are first and second level approximation components, respectively.

The approximation component (Y_a) contains the image components of low frequency while the detailed components (Y_h, Y_v and Y_d) contain high frequency components. Thus,

$$Y=Y^1_a+\{\ Y^1_h, +Y^1_v + Y^1_d\ \}. \quad (6)$$

If DWT is applied to Y^1_a, the second level approximation and detailed components are obtained. Likewise, decomposition at the Higher-level is performed. If the process is repeated to N levels, the image Y can be written in terms of the Nth approximation component (Y^N_a) and all detailed components as given below in Eq.(7),

$$Y=Y^N_a+\sum_{i=1\ to\ N}\{\ Y1h, +Y1v\ +\ Y1d\ \}. \quad (7)$$

The level of decomposed signals at each level of decomposition is half the length of the signal in the preceding step. Hence, the size of the approximation component obtained from the first level of N x N image decomposition is N/2xN/2, second level is N/4xN/4 and so on. A compact, but coarser approximation of the image is obtained as the level of decomposition increases. Wavelets, therefore, provide a simple hierarchical structure for interpreting image information.

D. Feature Reduction using PCA

The high dimensional feature vector prompts to high computational overhead and high space for storage. The application of techniques for the reduction of dimensionality is therefore of great importance. PCA has been found to be effective in reducing feature dimension that transforms high dimensional input data into a lower dimensional space while keeping maximum data variations [21, 22]. As mentioned above, the number of extracted features was reduced from 65536 to 1024.It is still too large to measure, though. Therefore, PCA is used to further minimize the size of features to a higher degree. Figure 4 shows the curve of cumulative sum of variance versus the number of principle components. Table 3 list the variances

TEST Engineering & Management

January - February 2020
ISSN: 0193 - 4120 Page No. 11323 - 11332

versus the number of principle components from 1 to 20. This indicate that only 19 principle components (bold font in table), which is only 1.86% of the original features, will retain 95.4% of total variance.

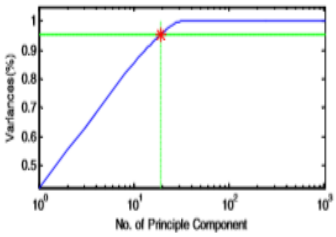

Figure 4. Variances against No. of principle components (x axis is log scale).

Table detailed data of PCA

No. of Prin. Comp.	1	2	3	4	5	6	7	8	9	10
Variance (%)	42.3	55.6	62.4	68.1	72.3	76.2	79.3	82.1	84.0	85.6
No. of Prin. Comp.	11	12	13	14	15	16	17	18	**19**	20
Variance (%)	87.3	88.6	89.8	91.0	92.0	93.0	93.9	94.6	**95.4**	96.1

E. Least Square Support vector machine (LS-SVM)

The new feature vectors and their class labels will be fed to the classifier for disease prediction after feature reduction. The conventional SVM does not do well on the large datasets when validating. On the other hand, it highly increases the complexity of computations greatly. Therefore, an efficient SVM variant called as least squares SVM (LS-SVM) has been deployed here to alleviate this computational overhead and improve the accuracy of the classification. In addition, it solves a series of linear equations due to the presence of equality type constraints in the formulation of LS-SVM; where as conventional SVM solves a quadratic programming problem [23]. For better understanding a brief description on LS-SVM is given here.

Let $\{p_i, y_i\}_{i=1}^{N}$ be a training set of N samples with input data $p_i \in R^m$ and class labels $y_i = \{-1, +1\}$, then LS-SVM is defined as the following optimization problem,

$$\underset{a,b,er}{min}\ J(a, b, e_r) = \frac{1}{2} a^T a + C \frac{1}{2} \sum_{i=1}^{N} e^2_{ri} \quad (8)$$

Subject to the equality constraint

$$y_i \{ a^T \varphi(pi) + b \] = 1 - e_{ri},\ i = 1, 2, ..., N \quad (9)$$

Here, φ (.) and *a* denotes the mapping function and the weight vector, respectively. The factor for regularization is C > 0. The bias term and the error variables are defined by *b* and e_{ri} , respectively.

we can express the Lagrangian for a set of Lagrange multipliers λ_i, as

$$L(a, b, e_r, \lambda) = J(a, b, e_r) - \sum_{i=1}^{N} \lambda_i \{ y_i [a^T \varphi(p_i) + b] - 1 + e_{ri} \} \quad (10)$$

The conditions for optimality are

$$\begin{cases} \frac{\partial L}{\partial a} = 0 \rightarrow a = \sum_{i=1}^{N} \lambda_i y_i \phi(p_i) \\ \frac{\partial L}{\partial b} = 0 \rightarrow \sum_{i=1}^{N} \lambda_i y_i = 0 \\ \frac{\partial L}{\partial e_{r_i}} = 0 \rightarrow \lambda_i = C e_{r_i}, \qquad i = 1, 2, \ldots, N \\ \frac{\partial L}{\partial \lambda_i} = 0 \rightarrow y_i [a^T \phi(p_i) + b] - 1 + e_{r_i} = 0, \ i = 1, 2, \ldots, N \end{cases}$$

which can be written as the solution to the following set of linear equations rather than quadratic equations

$$\begin{bmatrix} I & 0 & 0 & -ZT \\ 0 & 0 & 0 & -YT \\ 0 & 0 & CI & -I \\ Z & Y & I & 0 \end{bmatrix} \begin{bmatrix} a \\ b \\ er \\ \lambda \end{bmatrix} = \begin{bmatrix} 0 \\ 0 \\ 0 \\ 1 \end{bmatrix} \quad (11)$$

Where, $Z=[\varphi(P_1)^T y1;...;\varphi(P_N)^T y^N]$, $Y=[y_1;...;y_N]$, $I = [1;...; 1]$, $e_r = [e_{r1};...; e_{rN}]$, $\lambda = [\lambda_1;...; \lambda_N]$. The following solution can also be derived

$$\begin{bmatrix} 0 & -YT \\ Y & \Omega + C^{-1} I \end{bmatrix} \begin{bmatrix} b \\ \lambda \end{bmatrix} = \begin{bmatrix} 0 \\ 1 \end{bmatrix}$$

for $\Omega = ZZ^T$ and according to Mercer's condition [23],

$$\Omega_i k = y_i y_k \varphi(p_i)^T \varphi(p_k) = y_i y_k K(p_i, p_k) \quad (12)$$

The symbol K(., .) here represents the kernel function. Now, for a given K(., .) and a test sample p, the LS-SVM classifier is given by

$$f(p) = \text{sign} [\sum_{i=1}^{N} \lambda_i y_i K(p, p_i) + b] \quad (13)$$

The following types of kernels have been utilized in this paper for training the LS-SVM classifier.

– Linear: $K(p, p_i) = p^T{}_i\, p$

January - February 2020
ISSN: 0193 - 4120 Page No. 11323 - 11332

– Polynomial: $K(p, p_i) = (p^T{}_i\, p + 1)\delta$

– Radial basis function (RBF): $K(p, p_i) = \exp\{ -\|p - pi\|^2/2\sigma^2 \}$

where, parameter δ denotes the degree of the polynomial and kernel shape is controlled by a free parameter σ.

IV. EXPERIMENTAL DESIGN

A. Statistical setting

Usually, cross validation (CV) is used for the statistical test that has the advantage of solving over-fitting problems. It also lets the classifier generalize into independent datasets. Stratification is integrated into CV system to maintain approximately the same class distribution in each fold. This paper considers 5-fold stratified cross validation (SCV) for DS-66 and 5-fold SCV for rest two datasets. In addition, SCV method is repeated 10 times over three datasets in order to further avoid randomness. The three datasets used in our tests are set to SCV. 55 MR samples are used to train for the DS-66. Similarly, in the case of DS-160 and DS-255,128 and 204 samples are used for training, respectively. The validation samples are the samples which are not being used for training and therefore, the validation instances for DS-66, DS-160 and DS-255 are 11, 32, and 51 respectively.

B. Performance measures:

Three measures have been used to evaluate the efficiency of the suggested PBDS, namely, sensitivity (S_e), specificity (S_p), and accuracy. Note that we treat the pathological images are considered as positive class and healthy images as negative class. S_e is defined as the number of pathological MR images correctly predicted from the full set of pathological MR images, whereas S_p calculates the number of correctly predicted healthy MR images from the full set of healthy MR images. Accuracy is the total number of MR images that are predicted correctly.

C. Implementation

The implementation of suggested PBDS consists of two phases: offline learning and online evaluation where the first phase deals with classifier training using the large feature sets and the second one is utilized to estimate the new MR instances.

RESULTS AND COMPARISONS

With the help of Matlab image processing toolbox, the techniques were implemented in-house. The tests were conducted out on the Intel core processor, 4 GB RAM, and windows 10 OS.

D. Pre-processing results

CLAHE is used to enhance the low contrast MR images in the datasets chosen. The parameters of CLAHE are initialized as follows. For better enhancement the number of contextual regions is chosen as 64 by dividing the MR image by 8 in each direction equally. β is considered to be 0.01 which determines the limit for contrast enhancement limit and the number of bins used is set to 256, which is used in create a contrast enhancing transformation. To get a flat histogram shape for each region, the uniform distribution is chosen, which yields an efficient output. Two samples of brain MR (1 healthy and 1 pathological) with their enhanced output are shown in Fig. 5. The diseased-regions in the pre-processed images may be found to be more visible.

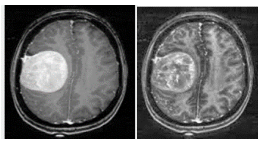

Figure 5 Brain MR image enhancement using CLAHE (β =0.01 and region size=8×8)

E. Segmentation results

The proposed PBDS uses a K means segmentation to segment the tumour edges in succession of pre-processing using CLAHE. Samples of brain MR (1 healthy and 1 pathological) with their segmented output are shown in Fig. 6.

January - February 2020
ISSN: 0193 - 4120 Page No. 11323 - 11332

Figure 6. Brain MR image segmentation using OTSU

F. Morphological operation results

After segmentation, Morphological operation is also used to calculate the area, size and density of the tumour. The results are shown in figure 7.

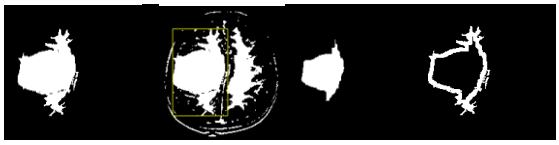

Figure 7. Brain MR image segmentation using a) tumor alone b) bounding box c) erode d)Tumor outline

G. Feature extraction results

Here, the number of DWT decomposition levels is set to 3 using (11) The top left corner of the wavelet coefficients image denotes the level-3 approximation coefficients, whose size is only 32×32 = 1024. Thus, it may be noted that only the coefficients of the selected sub-bands were used as features in our experiment. A healthy brain MR image with its coefficients at 5-level wavelet decomposition is shown in Fig. 3.

H. Feature reduction results

To simplify the model to reduce the training time, features need to be reduced and therefore, PCA is used. PCA has been applied to the combination of three datasets. The results obtained from PCA are shown in Fig. 8. It is evident that we retain more than 80 % of the cumulative variance with only six PCs. Here, we set the threshold line at 80 %, because the higher value of the threshold leads to more features and can increase the cost of computation.

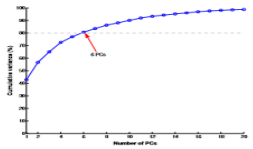

Figure 8. Plot between cumulative variance (%) and the number of PCs in PCA

I. Classification results

Certain classifiers such as KSVM, have been introduced to the show the effectiveness of the LS-SVM classifier. Note that for a valid comparison all the classifiers were implemented using the same features obtained from PCA. The comparisons show that performance yielded by LS-SVM + RBF is higher for three data sets among all classifiers.

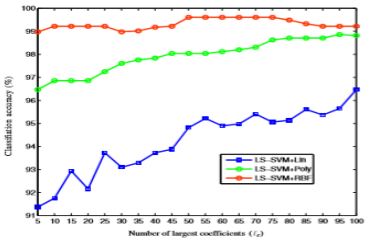

Figure 7. Overall classification accuracy with respect to lc over DS-255

Figure 7 shows the plots between l_c and the overall accuracies of three classifiers for DS-255.LS-SVM + RBF their accuracies are increased to 100 %, 100 %, and 99.61 %. To find out the optimal values of the parameters C and σ, we first set their ranges as C ∈ [1, 10] and σ ∈ [1, 100]. Then, different possible pairs of (C,σ) have been tested and finally the pair with the least SCV error was chosen. Similar tests have conducted to find the best value of δ (degree of the polynomial) where δ ∈ [1, 5]. Here, LS-SVM + Poly earns best performance for δ = 2; whereas LS-SVM + RBF offers best performance for σ = 1.

CONCLUSION

An efficient brain detection system is proposed in this paper. The proposed scheme first extracts DWT features from the pre-processed MR images of the brain an d then em-ploys a PCA technique to lower the hig h dimensional properties. Finally, a novel learning algorithm called LS-SLM is proposed to classify. The proposed scheme inherits the advantages of DWT and LS-SVM for detection of pathological brain from MR images. The proposed LS-SVM leaning algorithm has also been several advantages

January - February 2020
ISSN: 0193 - 4120 Page No. 11323 - 11332

over other learning algorithms like BPNN and conventional NN. The proposed PBDS has been validated on different accessible datasets, but its usefulness will be further illustrated by a larger online dataset. Moreover, deep learning algorithms could be investigated as the potential alternatives to the proposed LS-SVM.

REFERENCES

[1]. Y. Zhang, Z. Dong, et.al , "A hybrid method for MRI brain image classification", Expert Systems with Applications, vol. 38, no. 8, pp. 10049–10053, 2011.

[2]. S. Das, M. Chowdhury, and K. Kundu, "Brain MR image classification using multiscale geometric analysis of ripplet", Progress In Electromagnetics Research, vol. 137, pp. 1–17, 2013.

[3]. D. R. Nayak, et.al, "Brain MR image classification using two-dimensional discrete wavelet transform and AdaBoost with random forests", Neurocomputing, vol. 177, pp. 188–197, 2016.

[4]. ——, "Pathological brain detection using curvelet features and least squares SVM", Multimedia Tools and Applications, pp. 1–24, 2016.

[5]. E. A. El-Dahshan et.al, "Computer-aided diagnosis of human brain tumor through MRI: A survey and a new algorithm", Expert Systems with Applications, vol. 41, no. 11, pp. 5526–5545, 2014.

[6]. S. Chaplot et.al, "Classification of magnetic resonance brain images using wavelets as input to support vector machine and neural network", Biomedical Signal Processing and Control, vol. 1, no. 1, pp. 86–92, 2006.

[7]. E. S. A. El-Dahshan, et.al, "Hybrid intelligent techniques for MRI brain images classification", Digital Signal Processing, vol. 20, no. 2, pp. 433–441, 2010.

[8]. Y. Zhang, S. Wang, and L. Wu, "A novel method for magnetic resonance brain image classification based on adaptive chaotic PSO", Progress In Electromagnetics Research, vol. 109, pp. 325–343, 2010.

[9]. Y. Zhang, L. Wu, and S. Wang, "Magnetic resonance brain image classification by an improved artificial bee colony algorithm", Progress In Electromagnetics Research, vol. 116, pp. 65–79, 2011.

[10]. Y. Zhang, Z. Dong, et.al, "Magnetic resonance brain image classification via stationary wavelet transform and generalized eigenvalue proximal support vector machine", Journal of Medical Imaging and Health Informatics, vol. 5, no. 7, pp. 1395–1403, 2015.

[11]. Y. Zhang, Z. Dong, et.al, "Preclinical diagnosis of magnetic resonance (MR) brain images via discrete wavelet packet transform with Tsallis entropy and generalized eigenvalue proximal support vector machine", Entropy, vol. 17, no. 4, pp. 1795–1813, 2015.

[12]. X. Zhou, S. Wang, et.al, "Detection of pathological brain in MRI scanning based on waveletentropy and naive Bayes classifier", in Bioinformatics and Biomedical Engineering, 2015, pp. 201–209.

[13]. S. Wang, et.al, "Pathological brain detection by a novel image featurefractional Fourier entropy", Entropy, vol. 17, no. 12, pp. 8278–8296, 2015.

[14]. Y. Zhang, et.al, "Pathological brain detection based on wavelet entropy and Hu moment invariants", Bio-medical Materials and Engineering, vol. 26, no. s1, pp. S1283–S1290, 2015.

[15]. S. Wang, et.al, "Dualtree complex wavelet transform and twin support vector machine for pathological brain detection", Applied Sciences, vol. 6, no. 6, 2016.

[16]. Pisano ED, et.al (1998) "Contrast limited adaptive histogram equalization image processing to improve the detection of simulated spiculations in dense mammograms", J Digit Imag 11(4):193–200.

[17]. Pizer SM, et.al (1990) "Contrast-limited adaptive histogram equalization: speed and effectiveness", In: Proceedings of the first conference on visualization in biomedical computing. IEEE, pp 337–345

[18]. Reza AM (2004) "Realization of the contrast limited adaptive histogram equalization (CLAHE) for realtime image enhancement". VLSI Signal Process Syst Signal Image Vid Technol 38(1):35–44.

[19]. L. Dongju and Y. Jian, "Otsu method and k-means", in Hybrid Intelligent Systems, 2009. HIS

January - February 2020
ISSN: 0193 - 4120 Page No. 11323 - 11332

'09. Ninth International Conference on, vol. 1, 2009, pp. 344–349.

[20]. S. Chaplot, et.al, "Classification of magnetic resonance brain images using wavelets as input to support vector machine and neural network", Biomedical Signal Processing and Control, vol. 1, no. 1, pp. 86–92, 2006.

[21]. Duda RO, Hart PE, Stork DG (2012) Pattern classification.

[22]. Wiley, et.al, "Hybrid intelligent techniques for MRI brain images classification", Digital Signal Processing, vol. 20, no. 2, pp. 433–441, 2010.

[23]. Suykens JAK, Vandewalle J(1999) Least squares support vector machine classifiers.Neural Process Lett 9(3):293–300 .

[24]. Zhang Y, Wu L, Wang S (2011), "Magnetic resonance brain image classification by an improved artificial bee colony algorithm". Progress Electromagn Res 116:65–79

AUTHORS PROFILE

Dr.S.Nagaraja Rao, Professor & HOD of ECE dept., G.Pulla Reddy Engineering College (Autonomous), Kurnool, India. Received his Ph.D. degree from JNTUA, Anantapuramu, Andhra Pradesh, India in 2011. His area of interest is communication systems, Image & Signal processing. He is a professional member of ISTE and ISOI. He authorized for more than 50 papers in journals and conferences at international level.

M.Jayalakshmi, Research scholar, JNTUA, Anantapuramu, India. Received her M.Tech degree in the year 2010 from Sri Krishna Devaraya University, Anatapuramu, India. She is currently pursuing Ph.D. degree from JNTUA, Anantapuramu, and Andhra Pradesh. Her current research includes biomedical image processing.